doi:10.1093/brain/awx355 BRAIN 2018: 141; 888–902 | 888

BRAIN
A JOURNAL OF NEUROLOGY

Fibre-specific white matter reductions in Alzheimer's disease and mild cognitive impairment

Remika Mito,[1,2] David Raffelt,[1] Thijs Dhollander,[1] David N. Vaughan,[1,2,3] J.-Donald Tournier,[4,5] Olivier Salvado,[6] Amy Brodtmann,[1,2,7] Christopher C. Rowe,[8,9] Victor L. Villemagne[1,8,9] and Alan Connelly[1,2]

Alzheimer's disease is increasingly considered a large-scale network disconnection syndrome, associated with progressive aggregation of pathological proteins, cortical atrophy, and functional disconnections between brain regions. These pathological changes are posited to arise in a stereotypical spatiotemporal manner, targeting intrinsic networks in the brain, most notably the default mode network. While this network-specific disruption has been thoroughly studied with functional neuroimaging, changes to specific white matter fibre pathways within the brain's structural networks have not been closely investigated, largely due to the challenges of modelling complex white matter structure. Here, we applied a novel technique known as 'fixel-based analysis' to comprehensively investigate fibre tract-specific differences at a within-voxel level (called 'fixels') to assess potential axonal loss in subjects with Alzheimer's disease and mild cognitive impairment. We hypothesized that patients with Alzheimer's disease would exhibit extensive degeneration across key fibre pathways connecting default network nodes, while patients with mild cognitive impairment would exhibit selective degeneration within fibre pathways connecting regions previously identified as functionally implicated early in Alzheimer's disease. Diffusion MRI data from Alzheimer's disease ($n = 49$), mild cognitive impairment ($n = 33$), and healthy elderly control subjects ($n = 95$) were obtained from the Australian Imaging, Biomarkers and Lifestyle study of ageing. We assessed microstructural differences in fibre density, and macrostructural differences in fibre bundle morphology using fixel-based analysis. Whole-brain analysis was performed to compare groups across all white matter fixels. Subsequently, we performed a tract of interest analysis comparing fibre density and cross-section across 11 selected white matter tracts, to investigate potentially subtle degeneration within fibre pathways in mild cognitive impairment, initially by clinical diagnosis alone, and then by including amyloid status (i.e. a positive or negative amyloid PET scan). Our whole-brain analysis revealed significant white matter loss manifesting both microstructurally and macrostructurally in Alzheimer's disease patients, evident in specific fibre pathways associated with default mode network nodes. Reductions in fibre density and cross-section in mild cognitive impairment patients were only exhibited within the posterior cingulum when statistical analyses were limited to tracts of interest. Interestingly, these degenerative changes did not appear to be associated with high amyloid accumulation, given that amyloid-negative, but not positive, mild cognitive impairment subjects exhibited subtle focal left posterior cingulum deficits. The findings of this study demonstrated a stereotypical distribution of white matter degeneration in patients with Alzheimer's disease, which was in line with canonical findings from other imaging modalities, and with a network-based conceptualization of the disease.

1 Florey Institute of Neuroscience and Mental Health, Melbourne, Victoria, 3084, Australia
2 Florey Department of Neuroscience and Mental Health, University of Melbourne, Melbourne, Victoria, 3084, Australia
3 Department of Neurology, Austin Health, Heidelberg, Victoria, 3084, Australia
4 Department of Biomedical Engineering, Division of Imaging Sciences and Biomedical Engineering, King's College London, London, WC2R 2LS, UK
5 Centre for the Developing Brain, King's College London, London, WC2R 2LS, UK
6 CSIRO, Health and Biosecurity, The Australian eHealth Research Centre, Brisbane, Queensland, 4029, Australia

Received May 16, 2017. Revised October 19, 2017. Accepted November 8, 2017. Advance Access publication January 4, 2018

7 Eastern Clinical Research Unit, Monash University, Box Hill Hospital, Melbourne, Victoria, 3128, Australia
8 Department of Medicine, Austin Health, University of Melbourne, Heidelberg, Victoria, 3084, Australia
9 Department of Molecular Imaging and Therapy, Austin Health, Heidelberg, Victoria, 3084, Australia

Correspondence to: Remika Mito
Florey Institute of Neuroscience and Mental Health, 245 Burgundy Street, Heidelberg, Victoria 3084, Australia
E-mail: remika.mito@florey.edu.au

Keywords: Alzheimer's; diffusion; MRI; fixel; white matter

Abbreviations: AIBL = Australian Imaging, Biomarkers and Lifestyle study of aging; DTI = diffusion tensor imaging; DWI = diffusion-weighted imaging; FBA = fixel-based analysis; FDC = fibre density and cross-section; FOD = fibre orientation distribution; MCI = mild cognitive impairment

Introduction

Historically, Alzheimer's disease has been pathologically defined by the aggregation of abnormal amyloid-β and hyperphosphorylated tau proteins. The accumulation of amyloid-β has long been thought to play a precipitating role in disease pathogenesis, driving the pathological tau deposition and subsequent neurodegeneration that begins in the medial temporal lobe and later progresses throughout vulnerable neocortical regions (Hardy and Selkoe, 2002; Jack *et al.*, 2010). This neurodegeneration, in turn, initially manifests as a primary amnestic syndrome, and later as widespread cognitive impairment as other domains are impaired by disease spread. However, PET imaging studies have shown that amyloid-β deposition commonly occurs in elderly people with normal cognition (Mintun *et al.*, 2006; Aizenstein *et al.*, 2008), while deposition patterns show no, or at best weak, correlations with clinical disease syndromes (Rabinovici *et al.*, 2008; Rowe *et al.*, 2010; Leyton *et al.*, 2011; Rodrigue *et al.*, 2012). Furthermore, therapeutic interventions that have focused upon reducing levels of amyloid-β to lessen their purported neurodegenerative effects have been largely ineffective (Castellani and Perry, 2012; Giacobini and Gold, 2013).

While molecular pathologies are undoubtedly critical aspects of Alzheimer's disease aetiology, a valuable way to view the disease and target therapeutic interventions may be to consider the global, network-based dysfunctions that are characteristic to the disease (Palop *et al.*, 2006; Canter *et al.*, 2016). Network-based theories of Alzheimer's disease suggest that the disease selectively targets vulnerable regions and propagates across intrinsic networks in the brain, presumably via specific neuronal pathways (Frost and Diamond, 2010; Raj *et al.*, 2012; Zhou *et al.*, 2012). Functional neuroimaging evidence has played a crucial role in supporting theories of network-level susceptibility, showing characteristic patterns of disconnection between functionally connected, but not necessarily spatial adjacent brain regions that make up so-called intrinsic connectivity networks. In particular, the default mode network (DMN) has been implicated in Alzheimer's disease, and exhibits not only functional disconnection (Greicius *et al.*, 2004; Buckner *et al.*, 2009; Seeley *et al.*, 2009; Zhou *et al.*, 2012), but also metabolic disruptions (Minoshima *et al.*, 1997; Alexander *et al.*, 2002; Drzezga *et al.*, 2003; Nestor *et al.*, 2003), atrophy (Pengas *et al.*, 2010), and high amyloid-β accumulation (Buckner *et al.*, 2005). Functional network disruptions are likely to be subserved by changes to white matter fibre pathways making up the brain's structural networks, and the co-occurrence of molecular, metabolic, and functional changes could be explained by the presence of structural connections and their subsequent disruption, propagating network-wide failures. Investigating alterations within specific white matter fibre pathways would thus likely provide greater understanding of network-based changes over the course of Alzheimer's disease.

To this end, diffusion-weighted imaging (DWI) is currently the only method available to non-invasively study white matter fibre architecture *in vivo*, and has thus generated substantial interest, along with a rapidly increasing body of literature in its clinical applications. However, the value of DWI studies depends largely upon unbiased methods for data acquisition, pre- and post-processing of data, quantitative analysis, as well as careful interpretation of results (Jones *et al.*, 2013*b*). The vast majority of DWI studies investigating Alzheimer's disease have analysed DWI data based on the diffusion tensor model [diffusion tensor imaging (DTI)], and have performed quantitative comparisons using voxel-averaged metrics derived from this model, such as fractional anisotropy and mean diffusivity, which purport to reflect the structural integrity of white matter.

Over the past decade, numerous DTI studies have reported spatial and temporal changes in white matter that arise over the course of Alzheimer's disease, the results of which are summarized in a number of extensive reviews (Chua *et al.*, 2008; Sexton *et al.*, 2011; Gold *et al.*, 2012; Mak *et al.*, 2017). Despite promising results revealing white matter abnormalities in Alzheimer's disease, there are major shortcomings to DTI studies, which can render their findings to be both unreliable, and difficult to interpret biologically. A major limitation of the diffusion tensor is its limited ability to model complex and crossing-fibre populations, which have been shown to be present in up to 90% of white matter voxels (Jeurissen *et al.*, 2013). Accordingly,

when differences are detected in white matter voxels containing crossing-fibre populations, these are difficult to interpret or to assign to specific fibre pathways (Jones, 2010; Douaud *et al.*, 2011; Gold *et al.*, 2012; Jones *et al.*, 2013*b*). As such, while the voxel-averaged measures of tensor-derived metrics are sensitive to abnormalities within certain regions of white matter, they are inherently not fibre-specific nor easily interpretable, particularly in crossing-fibre voxels that constitute most of the brain's white matter.

Higher-order DWI models have enabled estimation of multiple fibre orientations within voxels (Tournier *et al.*, 2004, 2007; Assaf and Basser, 2005; Behrens *et al.*, 2007). To be sensitive to differences within specific fibre populations, it is important not only to estimate the orientations of each fibre population, but additionally to make use of quantitative metrics that independently characterize any degenerative changes to specific fibre populations within voxels. Doing so facilitates fibre tract-specific comparisons, as opposed to analyses of voxel-averaged metrics.

A recent technique that enables fibre tract-specific statistical analysis is fixel-based analysis (FBA) (Raffelt *et al.*, 2017), whereby a 'fixel' refers to a specific fibre population within a voxel (Raffelt *et al.*, 2015). FBA is based on the analysis of DWI data using constrained spherical deconvolution (Tournier *et al.*, 2007), which enables characterization of multiple fibre orientations within voxels. Using this approach, we can compare measures related to the total intra-axonal volume of white matter axons in any particular direction, thus providing a method that can be used to detect degeneration within specific white matter tracts. In a disease like Alzheimer's, which is associated with substantial brain atrophy, it is important to account for the potential morphological changes that may contribute to observed differences in group comparisons, as well as within-voxel microstructural differences. To this end, FBA can be used to estimate: (i) differences in the density of fibres within a fibre bundle; (ii) differences in the fibre-bundle cross-section; or (iii) differences arising from a combination of both degenerative processes (Fig. 1) (Raffelt *et al.*, 2017).

In this cross-sectional study, we describe the first application of FBA to a cohort of participants clinically diagnosed with mild cognitive impairment (MCI, $n = 33$) and Alzheimer's disease ($n = 49$). The aim of this study was to investigate if Alzheimer's disease is indeed characterized by a stereotypical pattern of white matter degeneration, and if early signs of specific fibre tract degeneration are apparent in MCI patients, who represent a somewhat heterogeneous cohort at-risk for Alzheimer's disease. We additionally investigated if early fibre tract degeneration differed between MCI patients without amyloid-β accumulation to those with high amyloid-β accumulation, who likely represent a prodromal Alzheimer's disease cohort. Our findings support theories of network-wide disruptions in Alzheimer's disease, and exhibit the value of implementing a fibre-specific method to investigate white matter degeneration *in vivo*.

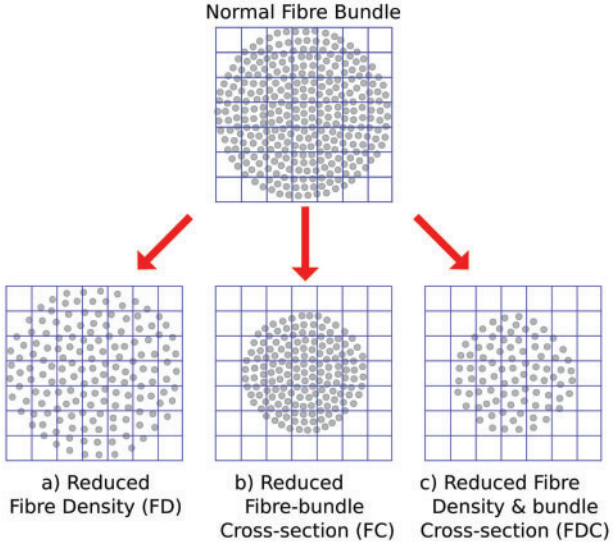

Figure 1 Fixel-based metrics. The schematic represents a fibre bundle cross-section (grey circles represent axons, while the grid represents imaging voxels). A change to the intra-axonal volume may manifest as: (a) difference in tissue microstructure that result in a change in within-voxel fibre density; (b) a macroscopic difference in a fibre bundle's cross-section; or (c) difference in a combination of both fibre density and bundle cross-sectional area. Figure republished with permission of Neuroimage; permission conveyed through Copyright Clearance Centre, Inc.

Materials and methods

Participants

Participants included patients with clinical Alzheimer's disease, MCI, and healthy elderly control subjects, all of whom were recruited as part of the Australian Imaging, Biomarkers and Lifestyle (AIBL) study of ageing. Alzheimer's disease and MCI subjects were recruited from memory disorder clinics or by geriatricians, psychiatrists, and neurologists. Healthy control participants were recruited through community advertisement. All participants were classified into clinical groups according to AIBL criteria, as has been previously described (Ellis *et al.*, 2009). In brief, all Alzheimer's disease patients met NINDS-ADRDA (National Institute of Neurological and Communicative Disorders and Stroke and Alzheimer's Disease and Related Disorders Association) diagnostic criteria for probable Alzheimer's disease, while MCI participants were classified by a clinical review panel as per internationally agreed criteria (Petersen *et al.*, 1999; Winblad *et al.*, 2004). Healthy control participants exhibited no cognitive impairment and satisfied inclusion and exclusion criteria detailed in Ellis *et al.* (2009). All participants also underwent an amyloid-β PET scan with ^{11}C-PiB (carbon-11-labelled Pittsburgh compound B). Amyloid-β positivity was defined as previously described by Rowe *et al.* (2013), using a mean standardized uptake value ratio (SUVR) across the neocortex over a cut-off value of 1.4. Individuals were classified as amyloid-positive (SUVR $\geqslant$ 1.4) or negative (SUVR $<$ 1.4). Participants with a clinical Alzheimer's disease diagnosis, but who were amyloid-negative ($n = 3$),

were excluded from this study, while both amyloid-positive and -negative MCI and healthy elderly control participants were included. The final cohort included 177 subjects: 95 healthy control subjects (31 amyloid-positive, and 64 negative), 33 subjects with MCI (20 amyloid-positive and 13 negative), and 49 Alzheimer's disease subjects. A summary of clinical and demographic data is available in Table 1. All subjects provided informed written consent, and the study was approved by the ethics committee at Austin Health.

Image acquisition and preprocessing

MRI data were acquired using a 3 T Siemens Tim Trio system (Siemens), with a 12-channel head coil receiver. DWI was performed with the following parameters: 60 axial slices, repetition time/echo time = 9200/112 ms, 2.3 mm isotropic voxels, 128 × 128 acquisition matrix, acceleration factor = 2. Sixty diffusion-weighted images (b = 3000 s/mm^2), and five volumes without diffusion weighting (b = 0 s/mm^2), were obtained with echo planar imaging. The DWI acquisition time was ∼9 min. A 3D MPRAGE (magnetization prepared rapid acquisition gradient echo) image (voxel size 1.2 × 1 × 1 mm, repetition time/echo time = 2300/2.98, flip angle = 9°) was also obtained from each subject, and was used to compute intracranial volume using SPM8.

Preprocessing of diffusion-weighted images included denoising of data (Veraart *et al.*, 2016), eddy-current correction and motion correction (Andersson and Sotiropoulos, 2016), bias field correction (Tustison *et al.*, 2010), and up-sampling DWI spatial resolution by a factor of 2 in all three dimensions using cubic b-spline interpolation, to a voxel size of 1.15 mm^3 (Raffelt *et al.*, 2012*b*). Intensity normalization across subjects was performed by deriving scale factors from the median intensity in select voxels of white matter, grey matter, and CSF in b = 0 s/mm^2 images, then applying these across each subject image. All preprocessing steps were conducted using commands either implemented within MRtrix3 (www.mrtrix.org), or using MRtrix3 scripts that interfaced with external software packages.

Following these preprocessing steps, fibre orientation distributions (FODs) were computed using Single-Shell, 3-Tissue Constrained Spherical Deconvolution (SS3T-CSD), with group averaged response functions for white matter, grey matter, and CSF (Dhollander and Connelly, 2016; Dhollander *et al.*, 2016). Spatial correspondence was achieved by first generating a group-specific population template with an iterative registration and averaging approach (Raffelt *et al.*, 2011) using FOD images from 30 subjects (10 Alzheimer's disease, 10 MCI, and 10 healthy control subjects). Each subject's FOD image was then registered to the template via a FOD-guided non-linear registration (Raffelt *et al.*, 2011, 2012*a*).

A tractogram was generated using whole-brain probabilistic tractography on the population template. Twenty million streamlines were first generated, and these were subsequently filtered to 2 million streamlines using the SIFT (spherical-deconvolution informed filtering of tractograms) algorithm (Smith *et al.*, 2013) to reduce reconstruction biases.

Fixel-based metrics

We derived metrics of apparent fibre density, fibre-bundle cross-section, and a combined measure of fibre density and cross-section (FDC) for each subject across all white matter fixels. Detailed methodology for FBA, along with interpretations for fixel-based metrics have been described by Raffelt *et al.* (2017). These are summarized in brief below.

Fibre density

We used the Apparent Fibre Density framework to compute a measure related to the intra-axonal restricted compartment at each fixel (Raffelt *et al.*, 2012*b*). According to this framework, a quantitative measure of fibre density can be derived from FOD images, given that the integral of the FOD along a particular direction is proportional to the intra-axonal volume of axons aligned in that direction. The fibre density measure is therefore specifically sensitive to alterations at a microstructural, within-voxel level (see Fig. 1). The fibre density value

Table 1 Clinical and demographic data of participants

	HC *n* = 95	MCI *n* = 33	AD *n* = 49	Statistic
Age, years (SD)	78.3 (7.5)	79.4 (7.6)	77.4 (8.2)	$F = 0.68$ $P = 0.51$
Males (%)	45 (47.4)	16 (48.5)	22 (44.9)	$\chi^2 = 0.12$ $P = 0.94$
^{11}C-PIB positivity (%)	31 (32.6)	20 (60.6)	49 (100[a])	$\chi^2 = 60.0$ $P < 0.001$
ICV (SD)	1432.6 (134.4)	1420.5 (158.6)	1403.0 (137.0)	$F = 0.76$ $P = 0.47$
Years of education (SD)	15.0 (9.5)	13.0 (3.7)	12.8 (3.7)	$F = 1.87$ $P = 0.16$
CDR (SD)	0 (0.1)	0.5 (0.3)	1.3 (0.7)	$F = 103.0$ $P < 0.001$
MMSE (SD)	28.6 (1.4)	26.6 (2.4)	18.2 (7.3)	$F = 55.4$ $P < 0.001$

Data are presented as mean (SD) or number (%). Reported *P*-values from one-way between-groups ANOVA for age and intracranial volume, and chi-square test for independence for sex and ^{11}C-PIB positivity. AD = Alzheimer's disease patients; CDR = clinical dementia rating; ^{11}C-PIB = carbon-11-labelled Pittsburgh compound B; HC = healthy elderly control subjects; ICV = intracranial volume (cm^3); MMSE = Mini-Mental State Examination.

[a]Note that ^{11}C-PIB positivity was an inclusion criterion for the Alzheimer's disease group.

was obtained by estimating each fixel's contribution to the total DWI signal in a voxel using SS3T-CSD (Dhollander and Connelly, 2016). Following spatial normalization, the fibre density value for each fixel in each subject was then assigned to a fixel template mask. In this way, the fibre density metric in corresponding fixels could be compared across groups.

Fibre bundle cross-section

While fibre density enables estimation of differences in intra-axonal volume of a fibre pathway within a voxel, another likely scenario is that a loss of axons results in atrophy of a fibre bundle across its entire cross-section (Fig. 1). Atrophy of a fibre pathway could mean that the spatial extent occupied by that bundle decreases, resulting in a macrostructural, morphological change. The fibre bundle cross-section metric was computed to be sensitive to such a change, as described by Raffelt *et al.* (2017). Briefly, morphological differences in the fixel cross-section (in the plane perpendicular to the fixel direction) were estimated for each fixel by using the non-linear warps to compute the change in fibre bundle cross-section required to spatially normalise the subject image to the template image. With respect to the template frame of reference, fibre bundle cross-section values >1 indicate a larger fibre cross-section in the subject, while fibre bundle cross-section values <1 indicate a smaller cross-section.

Fibre density and cross-section

Given that group differences may manifest as changes to both within-voxel fibre density and macrostructural changes in fibre-bundle cross-section (Fig. 1), we additionally computed a metric that combined both sources of information, namely the combined measure of FDC (Raffelt *et al.*, 2017).

Voxel-based analysis of tensor-derived metrics

The most common method to date to investigate changes in so-called measures of 'white matter integrity' is using voxel-wise analyses of tensor-derived metrics, most commonly fractional anisotropy and mean diffusivity. Therefore, in addition to the fibre tract-specific fixel-based metrics that constitute the primary results in the present work, we also performed voxel-based analysis of fractional anisotropy and mean diffusivity measures derived from application of the tensor model to the same diffusion MRI data used for fixel-based analysis. The methodology is described in detail in Supplementary material; however, in brief, fractional anisotropy and mean diffusivity were derived at each voxel per subject, and warped to the population template space using warps derived for fixel-based analysis. Voxel-based analysis was then performed with threshold-free cluster enhancement (Smith and Nichols, 2009) to determine if there were any significant group differences in either fractional anisotropy or mean diffusivity.

Statistical analysis

Whole-brain fixel-based analysis

To identify regions with altered fibre density, fibre bundle cross-section, and FDC in the Alzheimer's disease and MCI groups, we first compared metrics using whole-brain fixel-based analysis. Herein, we use the term 'whole-brain fixel-based analysis' or 'whole-brain FBA' to refer to a comparison of all white matter fixels identified within the brain. Statistical comparisons of fibre density, fibre bundle cross-section, and FDC between groups were performed at each white matter fixel by a General Linear Model, comparing (i) Alzheimer's disease versus controls; and (ii) MCI versus controls. Age and intracranial volume were included as nuisance covariates. Connectivity-based smoothing and statistical inference was performed using connectivity-based fixel enhancement (CFE), using 2 million streamlines from the template tractogram, and with default smoothing parameters (smoothing = 10 mm full-width at half-maximum, C = 0.5, E = 2, H = 3) (Raffelt *et al.*, 2015). Note that in CFE, smoothing is preferentially applied along structurally connected fixels, ensuring that fixel-based metrics are locally smoothed with fixels belonging to the same fibre tract. Family-wise error (FWE)-corrected *P*-values were then assigned to each fixel using non-parametric permutation testing over 5000 permutations (Nichols and Holmes, 2002).

Significant fixels (FWE-corrected *P*-value < 0.05) were then displayed using the *mrview* tool in MRtrix3. To better appreciate the fibre pathways implicated, significant fixels were displayed on the template-derived tractogram, in which streamlines were cropped to only those fixels that were significant. Significant streamlines were colour-coded either by streamline orientation (left-right: red, inferior-superior: blue, anterior-posterior: green), or by the effect size expressed as a percentage relative to the control group. Both whole-brain fixel-based statistical analyses and visualizations were performed in MRtrix3.

Tract of interest analysis

We performed further tract of interest analyses to investigate potential degeneration of selective fibre pathways in MCI participants, who were potentially at risk of later developing Alzheimer's disease. We selected all fixels that exhibited statistically significant decreases in the FDC metric in the Alzheimer's disease group upon whole-brain FBA, and categorized these fixels into 11 white matter tracts, using anatomical DTI atlases to guide categorization (Wakana *et al.*, 2004; Mori *et al.*, 2005; Oishi *et al.*, 2009; Zhang *et al.*, 2010). Mean FDC was computed across the fixels in each defined tract—namely, the bilateral uncinate fasciculi, inferior fronto-occipital fasciculi (IFOF), anterior cingulum and posterior cingulum, the genu and splenium of the corpus callosum, and left arcuate fasciculus—and compared across groups.

Two tract of interest analyses were performed: (i) comparing across the diagnostic groups (Alzheimer's disease and MCI, to healthy control subjects as per whole-brain FBA); and (ii) a follow-up analysis incorporating amyloid-β status to determine potential association of amyloid accumulation with white matter degeneration [Alzheimer's disease ($n = 49$), amyloid-positive MCI ($n = 20$), amyloid-negative MCI ($n = 13$), and amyloid-positive healthy subjects ($n = 31$), compared to amyloid-negative healthy control subjects ($n = 64$)]. Statistical comparison was performed with a linear mixed model (with age, sex, and intracranial volume as covariates), using a Dunnett correction for multiple group comparisons in R software (*multcomp* package). A Bonferroni correction was performed for the 11 tracts (multiplying the *P*-value by a factor of 11). A significance threshold of 0.05 was used. Results were displayed

as the mean FDC and 95% confidence interval (CI) for each group, as a percentage difference from the mean FDC of the control group.

Results

Clinical and demographic characteristics

Clinical and demographic characteristics of each diagnostic group are summarized in Table 1. Patient and control groups did not significantly differ in age, sex, years of education or intracranial volume. Age histograms for each group are available in Supplementary Fig. 1.

Whole-brain fixel-based analysis

Figure 2 shows streamline segments associated with fixels that had a significant (FWE-corrected P-value < 0.05) decrease in the Alzheimer's disease group, for fibre density, fibre bundle cross-section, and FDC. Streamlines are coloured by the magnitude of reductions in Alzheimer's disease patients compared to control subjects. Large decreases in microstructural fibre density were observed across specific fibre pathways, with some fibre pathways (such as the parahippocampal cingulum) exhibiting fibre density decreases of $>40\%$ in Alzheimer's disease patients compared to control subjects. Macrostructural decreases in fibre bundle cross-section were less pronounced, though more spatially extensive. While macrostructural fibre bundle cross-section and microstructural fibre density differences overlapped across some fibre tracts, macrostructural differences were more apparent across long association fibres such as the cingulum bundle, superior and inferior longitudinal, and arcuate fasciculi, while commissural fibres and short association fibres, along with the IFOF, exhibited greater decreases in microscopic fibre density. Furthermore, some fibre pathways only exhibited decreases in fibre density, most notably the left fornix, while the superior longitudinal fasciculus exhibited decreases only in fibre bundle cross-section. When macro- and microstructural fibre differences were taken together using the FDC metric, the largest decreases in total intra-axonal volume occupied by fibre bundles were observed in posterior parietal white matter, the uncinate fasciculus, parahippocampal aspect of the cingulum bundle, and in the lateral aspects of the anterior commissure (Fig. 2). Figure 3 displays in greater detail streamline segments with significant FDC decreases in Alzheimer's disease patients. The 3D spatial distribution of affected fibre pathways for all three metrics can be appreciated in Supplementary Videos 1 and 2. As shown in Fig. 4, significant results within a voxel are specific to each fixel, even in crossing-fibre regions.

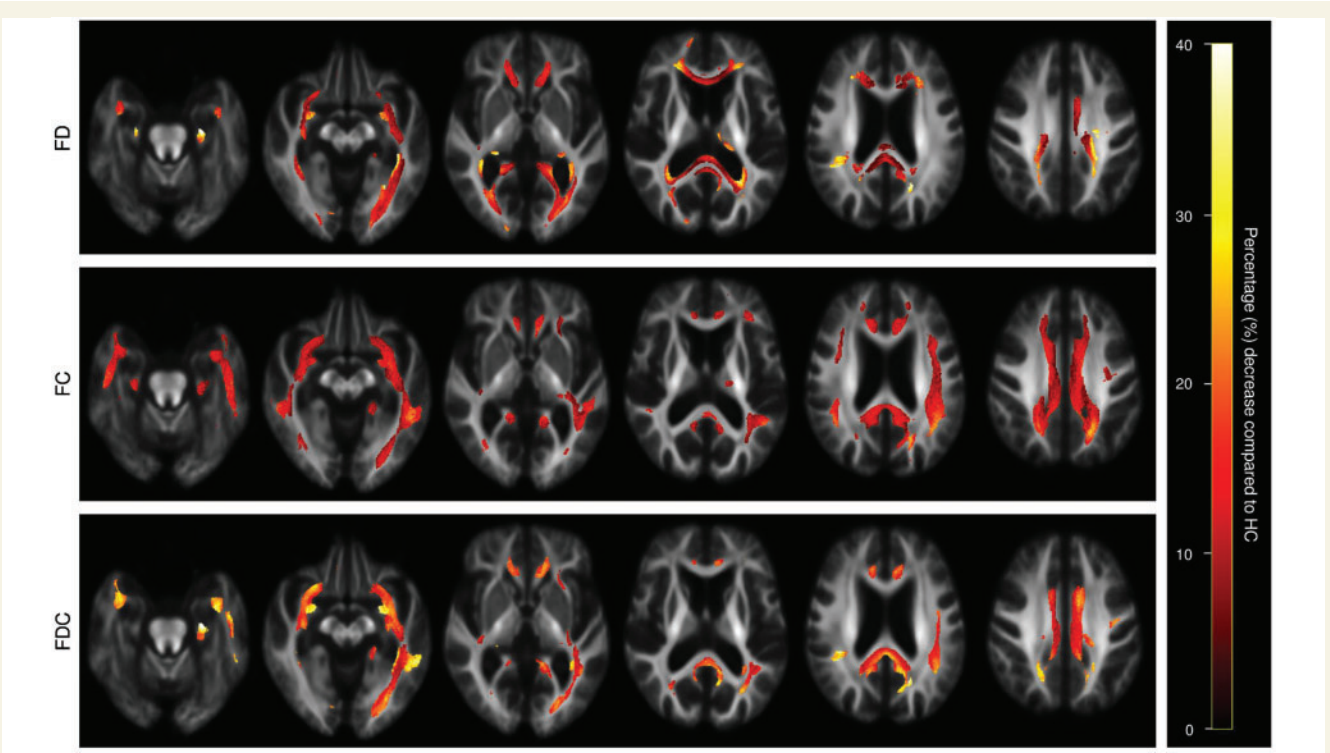

Figure 2 Fibre tract-specific reductions in Alzheimer's disease from whole-brain FBA. Streamline segments were cropped from the template tractogram to include only streamline points that correspond to significant fixels (FWE-corrected P-value < 0.05). Streamlines were coloured by percentage effect decrease in the Alzheimer's disease group compared to the healthy control group (HC) for fibre density (FD), fibre bundle cross-section (FC), and FDC. Significant streamlines are displayed across axial slices of the population template map.

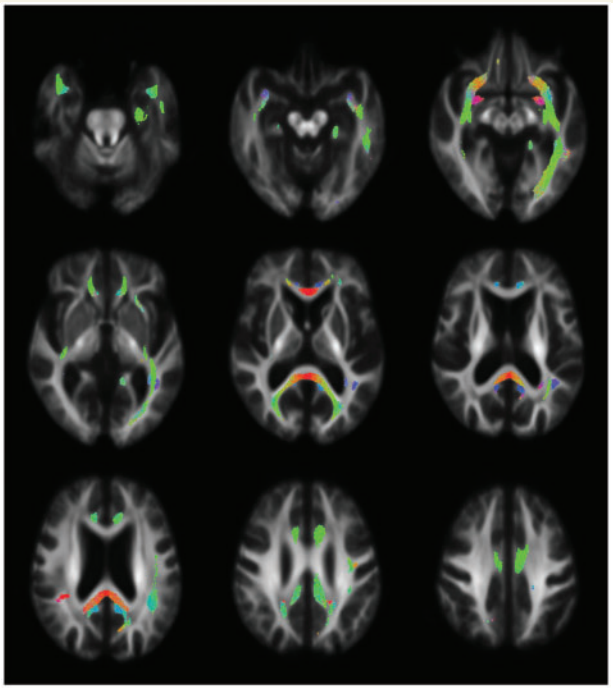

Figure 3 Fibre tract-specific significant FDC decreases in patients with Alzheimer's disease compared to healthy control subjects. Streamline segments were cropped from the template tractogram to include only those corresponding to fixels that exhibited a significant (FWE-corrected *P*-value < 0.05) decrease in the FDC metric in the Alzheimer's disease group. Significant streamline points are shown across a number of axial slices, and are coloured by direction (anterior-posterior: green; superior-inferior: blue; left-right: red).

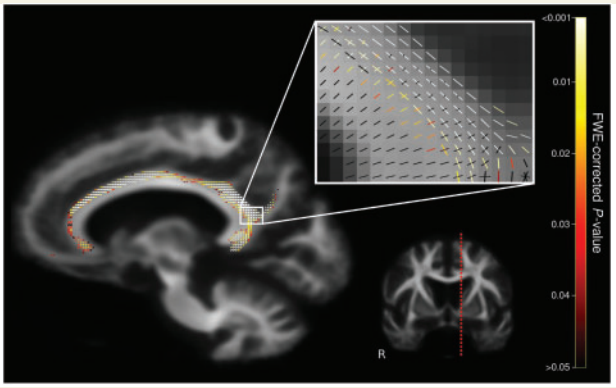

Figure 4 Fixel-based analysis enables fibre tract-specific analysis in crossing-fibre regions. Fixels that were significantly decreased in the Alzheimer's disease group compared to the healthy control group for the FDC metric are shown for a single sagittal slice (location shown on coronal section on *bottom right*). The zoomed insets exhibits differences to specific fixels in crossing-fibre regions, with fixels coloured by FWE-corrected *P*-value.

When MCI patients were compared to healthy controls with whole-brain FBA, no significant decreases were observed across any fixels for any of the three metrics.

Voxel-based analysis of tensor-derived metrics

Alzheimer's disease patients exhibited significant decreases in fractional anisotropy and significant increases in mean diffusivity across extensive white matter voxels, in line with previous reports (Supplementary Fig. 2). Additionally, significant fractional anisotropy increases were observed in Alzheimer's disease patients compared to control subjects within voxels known to contain crossing-fibre populations, in particular within the centrum semiovale (Fig. 5).

Tract of interest analysis

Comparison of fibre density and cross-section between clinical diagnostic groups

In the MCI group, significant decreases were apparent in the posterior cingulum bundle [left: $t(171) = -3.48$, $P = 0.001$, right: $t(171) = -2.50$, $P = 0.026$], and the right uncinate fasciculus [$t(171) = -2.31$, $P = 0.043$] only. Only the left posterior cingulum survived Bonferroni correction over the number of tracts investigated (corrected *P*-value = 0.014). No significant difference was found for the remainder of the tracts in the MCI group compared to controls (Fig. 6). Alzheimer's disease patients exhibited decreased FDC in all 11 white matter tracts upon tract of interest analysis, when compared to the healthy controls, as expected given that the tracts of interest were defined in terms of already being significantly different in this group upon whole-brain FBA.

Association of fibre density and cross-section differences with amyloid positivity

We explored further whether observed differences in MCI patients, as measured by decreases in FDC, were primarily in those individuals who also exhibited substantial amyloid-β accumulation. Comparing Alzheimer's disease, amyloid-positive MCI, amyloid-negative MCI, and amyloid-positive healthy subjects to amyloid-negative control subjects, we found significant decreases in FDC in the left posterior cingulum in the amyloid-negative MCI group only [$t(169) = -2.82$, $P = 0.02$]; however, this did not survive Bonferroni correction. Figure 7 shows that this group exhibited a trend toward lower FDC than the amyloid-positive MCI group across most of the remaining fibre pathways; however, this was not significant. No significant differences were found between amyloid-positive and negative healthy control subjects (Fig. 7). All 11 white matter tracts exhibited a significant decrease in tract of interest-based FDC in the Alzheimer's disease group compared to healthy control subjects without high amyloid accumulation, which is as expected given how these tracts of interest were defined.

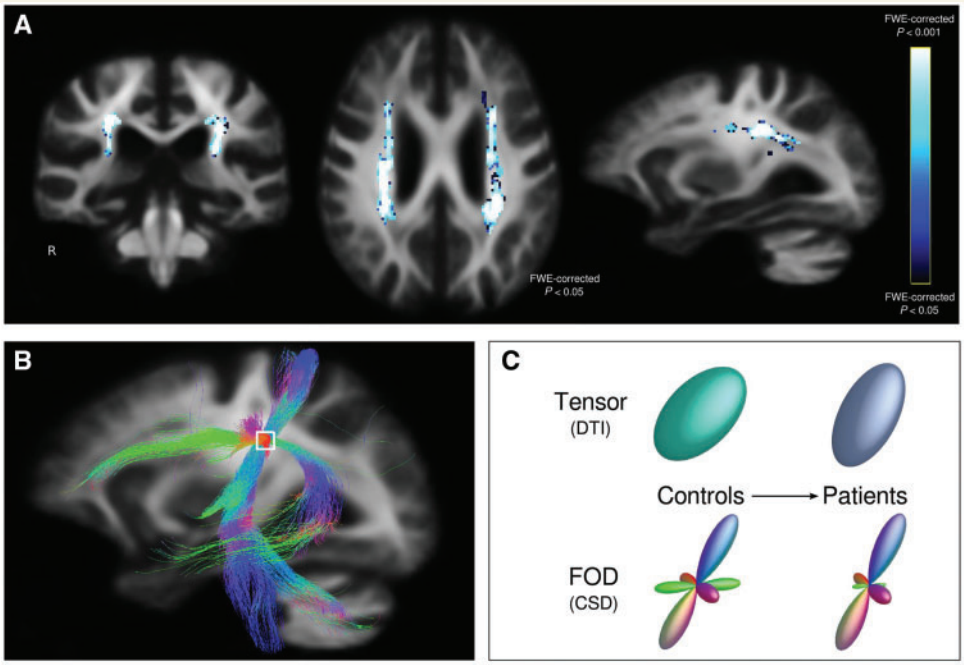

Figure 5 Significant voxel-wise increases in fractional anisotropy in Alzheimer's disease compared to healthy controls. (**A**) Voxels exhibit a significant (FWE-corrected *P*-value < 0.05) increase in fractional anisotropy in the Alzheimer's disease group compared to healthy controls along coronal, axial and sagittal views. (**B**) The centrum semiovale contains fibre structures belonging to the corticospinal tract, superior longitudinal fasciculus, and corpus callosum, as can be demonstrated with probabilistic tractography. Alzheimer's disease patients exhibited white matter degeneration specifically within the superior longitudinal fasciculus, with relative preservation of the corticospinal tract and body of the corpus callosum. (**C**) Using a DTI model this difference would be detected as an increase in fractional anisotropy, given that the relative contribution of the superior longitudinal fasciculus to the tensor is decreased, resulting in a misleading increase in anisotropy along the direction of the corticospinal tract. Modelling the equivalent voxel with a fibre orientation distribution function (FOD) derived using constrained spherical deconvolution (CSD), we can appropriately resolve the different fibre orientations within the voxel. Thus, we can detect a fixel-specific decrease in the fixel corresponding to the superior longitudinal fasciculus, without any significant abnormality in fixels belonging to the corticospinal tract and corpus callosum in the same voxel.

Discussion

In the present study, we applied a recently established method to investigate fibre tract-specific white matter changes in Alzheimer's disease and MCI. This comprehensive investigation of pathway-specific disruptions offers valuable findings pertaining both to Alzheimer's disease specifically, and to the investigation of white matter structural networks more broadly. The major disease-related findings of this study were that: (i) patients with Alzheimer's disease exhibit extensive axonal loss within specific fibre pathways, in line with network-based conceptualizations of the disease; and (ii) MCI patients exhibit subtle axonal reduction within the posterior cingulum, which does not appear to be associated with high amyloid-β accumulation.

Extensive axonal loss across characteristic fibre pathways in Alzheimer's disease

Application of novel fixel-based methodology to a cohort of patients with Alzheimer's disease enabled the identification of substantial fibre density and cross-sectional reductions within specific white matter structures. Fibre tract-specific atrophy (as indexed by the fibre bundle cross-section metric) was spatially extensive in Alzheimer's disease patients; however, greater effects were observed in microstructural fibre density reduction, suggesting substantial axonal loss occurs at a microstructural level in the presence of morphological alterations to white matter structures in the disease.

Our results indicated that selective degeneration arises along specific fibre pathways in patients with Alzheimer's disease; in particular, the cingulum bundle along its anterior, posterior, and parahippocampal aspects, the corpus callosum (splenium and genu), uncinate fasciculus, inferior fronto-occipital fasciculus, and arcuate fasciculus. These fibre pathways connect brain regions that have previously been described as functionally implicated in Alzheimer's disease, and thus, our findings provide support for a structural basis to theories of network-based degeneration.

In line with the functional neuroimaging literature, which suggests that network degeneration occurs selectively within intrinsic connectivity networks, particularly the DMN (Delbeuck *et al.*, 2003; Palop *et al.*, 2006;

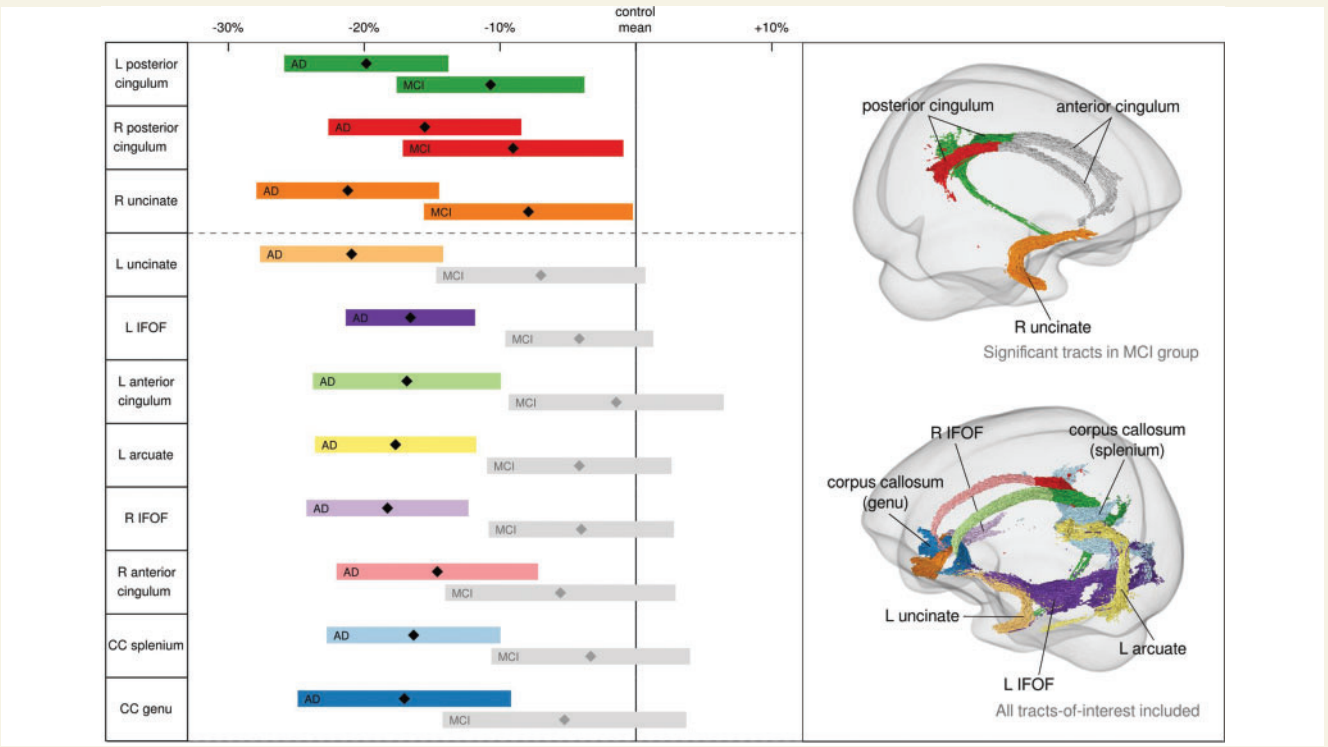

Figure 6 Significant tracts in MCI from tract-of-interest analysis comparing diagnostic groups. *Left*: Mean fibre density and cross-section (diamonds) and 95% CIs (bars) within tracts of interest are displayed for Alzheimer's disease (AD) and MCI groups, as a percentage difference from the healthy control mean, adjusted for age, sex, and intracranial volume. Significant tracts ($P < 0.05$) are displayed in colour, while non-significant are shown in grey. Results at the *top* (above dotted line) correspond to tracts where MCI patients were significantly different from healthy controls. *Right*: Tracts are shown in glass brain representations. *Top* brain shows tracts that were significantly altered in the MCI group, while *bottom* brain shows all tracts included in analysis, which all showed significant decrease in patients with Alzheimer's disease. Tracts are coloured to correspond with the *left* panel. Note that tracts were selected from significant fixels in the Alzheimer's disease group from the whole-brain FBA. Note also that for the MCI group, only the left posterior cingulum survived Bonferroni correction over the number of tracts tested. CC = corpus callosum; IFOF = inferior fronto-occipital fasciculus.

Zhou *et al.*, 2012; Brier *et al.*, 2014; Jones *et al.*, 2016), the white matter fibre pathways exhibiting fibre density and cross-sectional decreases in this cohort included those that likely form reciprocal connections between DMN regions. For example, the cingulum bundle is understood to form connections with and between the anterior medial prefrontal cortex, posterior cingulate cortex, and medial temporal lobe (van den Heuvel *et al.*, 2008; Greicius *et al.*, 2009; Jones *et al.*, 2013*a*). Additionally, structural disruption of the uncinate fasciculus would be consistent with functional disconnections within the ventral DMN; namely between the ventral medial prefrontal cortex and hippocampal formation, which this fibre pathway likely connects (Carmichael and Price, 1995; Wakana *et al.*, 2004; Petrides and Pandya, 2007). Disconnections within the genu of the corpus callosum could reflect the observed functional disruptions between the anterior medial prefrontal cortex bilaterally, while the splenium likely contributes homotopic connections between the posterior inferior parietal cortices, as well as the posterior cingulate and retrosplenial cortices (De Lacoste *et al.*, 1985; Teipel *et al.*, 2010). Degeneration of the inferior fronto-occipital fasciculus could also be associated with disconnections to DMN regions such as the angular gyrus to which it is believed to connect (Hau *et al.*, 2016). Degeneration to this fibre pathway may be closely related to vascular pathology and white matter hyperintensities as has been recently suggested (Taylor *et al.*, 2017).

The fibre tracts implicated in this present study were also largely congruent with the regions of white matter abnormalities reported in the extensive body of DTI literature (Rose *et al.*, 2000; Zhang *et al.*, 2007; Chua *et al.*, 2008; Nakata *et al.*, 2008; Villain *et al.*, 2008; Damoiseaux *et al.*, 2009; Acosta-Cabronero *et al.*, 2010; Sexton *et al.*, 2011; Agosta *et al.*, 2012; Bosch *et al.*, 2012). Moreover, our whole-brain voxel-based analyses of tensor-derived metrics were similarly in line with previous studies, with similar regions of white matter exhibiting decreased fractional anisotropy and increased mean diffusivity. However, it is important to highlight in this context that while the fixel-based results in this study overlap to some extent with regions identified in DTI findings both in the present study and in previous work, the fixel-based findings offer much greater anatomical specificity and biological interpretability by identifying tract-specific differences and accounting for the substantial atrophic changes that arise in the disease.

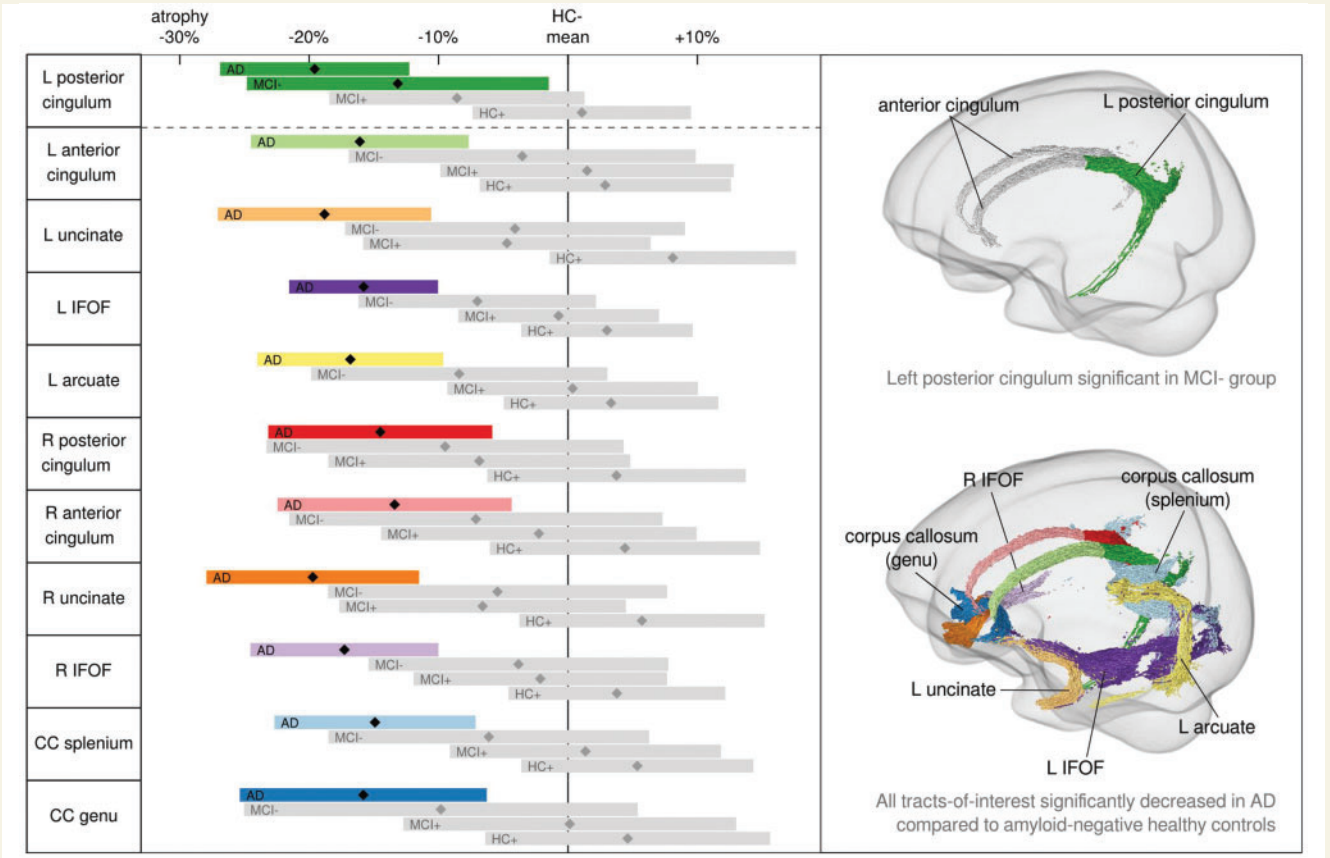

Figure 7 Group differences in mean FDC when including amyloid-β status. *Left*: Mean FDC (diamonds) and 95% CIs (bars) within tracts of interest are displayed for four groups: Alzheimer's disease (AD), amyloid-negative MCI (MCI−), amyloid-positive MCI (MCI+), and amyloid-positive healthy subjects (HC+). These are represented as a percentage difference from the control group; in this case, amyloid-negative healthy subjects (HC−). The left posterior cingulum was significantly decreased in the MCI− group ($P = 0.02$; did not survive Bonferroni correction). *Right*: *Top* glass brain shows the left posterior cingulum (green), which was significantly decreased in the MCI− group. *Bottom* glass brain shows all tracts, coloured according to the *left* panel, as per Fig. 6. CC = corpus callosum; IFOF = inferior fronto-occipital fasciculus.

Notably, the pathways affected in Alzheimer's disease patients were mostly long association fibres traversing between distant brain regions, which cross with other fibre pathways at many points along their length. This has precluded robust interpretation of DTI findings, as the orientation of underlying fibres cannot be reliably estimated using the diffusion tensor model. DTI metrics are inherently voxel-averaged, with the potential to be highly misleading in crossing-fibre regions (Jones *et al.*, 2013*b*). Indeed, previous studies have reported potentially misleading findings of increased anisotropy in disease cohorts in regions with crossing fibres, for example in the centrum semiovale (Douaud *et al.*, 2011) and along the cingulum bundle (Lee *et al.*, 2015). Similarly, here we observed regions of increased fractional anisotropy in Alzheimer's disease; in particular, the centrum semiovale exhibited increased fractional anisotropy (Fig. 5), while FDC decreases were observed within fixels belonging to the superior longitudinal fasciculus within this same region.

Tensor-based metrics are sensitive to diffusional properties that are averaged across a voxel, and thus the above-mentioned increases in fractional anisotropy in the centrum semiovale can be explained by the relative preservation of the corticospinal tract and corpus callosum, in the presence of degeneration of the superior longitudinal fasciculus. As illustrated in Fig. 5C, by modelling the underlying fibre structure using a FOD function derived from constrained spherical deconvolution (CSD), we can directly assess differences within specific fixels, even within crossing-fibre regions. In contrast, the tensor is sensitive at best to the voxel-averaged differences, which can potentially result in a highly misleading conclusion.

Subtle degeneration of the posterior cingulum in mild cognitive impairment

The posterior cingulate cortex has been implicated as a region affected early in the course of Alzheimer's disease, exhibiting hypometabolism (Minoshima *et al.*, 1997; Nestor *et al.*, 2003), and functional disruption (Greicius

et al., 2004; Zhou *et al.*, 2012), even in presymptomatic individuals who later go on to develop the clinical syndrome. The posterior aspect of the cingulum bundle likely constitutes short association fibres connecting regions of the posterior cingulate along with those that connect to structures of the temporal lobe (Jones *et al.*, 2013*a*; Wu *et al.*, 2016). Accordingly, our primary tract of interest analysis exhibited selective disruption within the left posterior cingulum in MCI patients. Large decreases were also observed in the right posterior cingulum and uncinate fasciculus; however, these were not significant following multiple comparison correction over the number of fibre bundles investigated. This finding could suggest that clinical MCI is associated with selective degeneration within fibre pathways that are later implicated in Alzheimer's disease. Indeed, our findings are consistent with previous DTI studies, which have similarly indicated early changes within the posterior cingulum in the progression of Alzheimer's disease (Fellgiebel *et al.*, 2005; Zhang *et al.*, 2007; Nakata *et al.*, 2008; Villain *et al.*, 2008).

It is important to note, however, that MCI is a clinical label, and the underlying pathology, as well as the clinical trajectory, can be heterogeneous (Petersen *et al.*, 1999; Larrieu *et al.*, 2002; Jicha *et al.*, 2006). While MCI subjects are at higher risk of progressing to Alzheimer's disease than cognitively unimpaired elderly individuals (Petersen, 2004; Gauthier *et al.*, 2006; Mitchell and Shiri-Feshki, 2009), only those MCI subjects who also exhibit a high amyloid-β accumulation are believed to represent a prodromal Alzheimer's disease cohort (Villemagne *et al.*, 2013).

Contrary to expectation, we found that the observed decrease in FDC in the left posterior cingulum in MCI patients was driven to a greater extent by those without high amyloid-β accumulation. Subtle degeneration to the left posterior cingulum was observed (significant only at an uncorrected level) in the MCI group without high amyloid-β accumulation, whereas MCI patients with high amyloid-β accumulation did not exhibit significant abnormalities in any of the investigated white matter tracts when compared to healthy elderly subjects without high amyloid-β accumulation.

Though a subtle result, this was seemingly contradictory to previous suggestions of the posterior cingulum as a critical pathway in the pathogenesis of Alzheimer's disease. Indeed, the posterior cingulum has been theorized to play an important role in early disease, connecting the amyloid-laden posterior cingulate cortex with the entorhinal and hippocampal regions, within which previously benign neurofibrillary changes are converted into an accelerated, degenerative tauopathy (Acosta-Cabronero *et al.*, 2010). Specific abnormalities within this fibre tract have also been suggested as a potential early predictor for the development of Alzheimer's disease (Zhang *et al.*, 2007; Nakata *et al.*, 2008). However, our findings suggest that specific degeneration of the posterior cingulum would not be a useful predictor for progression of MCI individuals to Alzheimer's disease, and that degeneration of this pathway is related to cognitive impairment irrespective of underlying pathology. The subtle posterior cingulum degeneration exhibited by the amyloid-β-negative MCI group in our study may be more closely associated to other pathological insults, such as white matter hyperintensities of presumed vascular aetiology, than to amyloid-β accumulation (Wardlaw *et al.*, 2013). These lesions were not accounted for in the present study, and future work would benefit from investigating the effects of other pathological insults in this pathologically heterogeneous clinical group.

Technical advantages of fixel-based analysis

The investigation of white matter degeneration in Alzheimer's disease and MCI is by no means a recent development (Brun and Englund, 1986; Englund *et al.*, 1988). DTI was a pioneering method that enabled investigation of microstructural changes to white matter *in vivo*, and was rapidly adopted as a potentially powerful method to investigate abnormalities in diseased individuals (Pierpaoli and Basser, 1996; Rose *et al.*, 2000; Taoka *et al.*, 2006). DTI studies have identified regions of purported microstructural abnormality, being highly sensitive to the diffusional properties of white matter. Voxel-based results of DTI studies have been extrapolated to suggest the likely fibre structures that may be implicated in Alzheimer's disease; however, the inherently voxel-based nature of these analyses precludes the ability to identify specific fibre pathways. Moreover, as has been demonstrated with our voxel-based fractional anisotropy analysis, there are limitations to using a voxel-based method when investigating complex white matter microstructure, which can result in misleading findings.

The most popular approach to perform diffusion tensor analyses is with Tract-Based Spatial Statistics (TBSS; Smith *et al.*, 2006). This method was developed to improve correspondence of fractional anisotropy images, and circumvent partial volume effects by projecting volumetric data onto a white matter 'skeleton'. However, the skeletonization and projection step discards orientational information from the diffusion data, and the method is not in fact 'tract-based' in reality. Moreover, there are major shortcomings to TBSS that have been described previously, and the results of TBSS analyses are often thought to be less biologically plausible and have decreased detection accuracy when compared to whole-brain voxel-based analyses (Jones *et al.*, 2013*b*; Bach *et al.*, 2014; Schwarz *et al.*, 2014; Raffelt *et al.*, 2015). With the advent of higher-order diffusion models, more recent studies have adopted novel tractographic approaches or crossing-fibre models to improve sensitivity to white matter changes in a more fibre tract-specific manner when performing voxel-based comparisons (Reijmer *et al.*, 2012; Wang *et al.*, 2016; Doan *et al.*, 2017). The major advantage to the present study however, is moving entirely beyond a tensor model that has inherently voxel-averaged comparisons, to

using a fibre tract-specific model and performing fixel-based comparison that provide more directly interpretable measures of structural connectivity.

Fixel-based analysis not only accounts for crossing-fibre populations, but additionally accounts for the differing ways in which changes to intra-axonal volume may manifest (Raffelt *et al.*, 2017). Accounting for both microstructural changes in density (with the fibre density metric), and macrostructural, morphometric changes (with the fibre bundle cross-section metric) enables a more comprehensive analysis of total intra-axonal volume changes within a fibre pathway (FDC metric) (Raffelt *et al.*, 2017). Indeed, in a disease like Alzheimer's, in which substantial white matter loss occurs (Brun and Englund, 1986), partial volume effects could contribute to significant findings in voxel-based analyses of white matter microstructure. As such, it is important to consider both microstructural and morphological differences that might reflect axonal loss.

Fixel-based analysis enables a more comprehensive insight into white matter changes, as illustrated by recent application in other disease states (Genc *et al.*, 2017; Raffelt *et al.*, 2017; Vaughan *et al.*, 2017; Wright *et al.*, 2017; Gajamange *et al.*, 2018). Here, we report the first application to an Alzheimer's disease and MCI cohort, which has offered novel perspectives into the degenerative changes to fibre pathways in both these clinical disease states.

Limitations and future directions

Despite these technical advantages, there are a number of limitations to our study. The cross-sectional study design limited our ability to describe white matter degenerative changes over the progression of MCI and Alzheimer's disease. Future studies investigating the longitudinal trajectory of MCI patients who progress to Alzheimer's disease is likely to provide further insight into the association of clinical trajectory with degenerative changes in particular fibre pathways.

Furthermore, in this study we did not exclude participants with other pathological insults that could potentially influence white matter degeneration in conjunction with the molecular neuropathological processes of Alzheimer's disease. In particular, white matter hyperintensities on MRI were apparent in many of the patients as well as healthy control subjects in our cohort, similar to previously reported cohorts (Yoshita *et al.*, 2006; Brickman, 2013; Thal *et al.*, 2014). The presence of these lesions has been associated with differences in tensor-derived metrics (Vernooij *et al.*, 2008; Altamura *et al.*, 2016), and is also likely to be associated with decreases in fixel-wise fibre density (Dhollander *et al.*, 2017). Future work will thus investigate the association of fibre density and cross-sectional differences with the presence of connected lesions.

While the diffusion imaging data acquired in our study were of high quality (particularly with regard to the number of gradient directions and b-value), a limitation of our data is that reverse-phase encoded images were not available for all our subjects, and as such, we could not perform correction for magnetic susceptibility-related image distortion. The absence of such correction could introduce greater variance in the fixel-based metrics, which could result in more conservative estimates of differences between groups.

One of the major unanswered questions regarding Alzheimer's disease is the means by which the various potential pathological insults that characterize the disease might contribute to its clinical and pathological progression. While the focus of the present work was to investigate tract-specific white matter connectivity differences in Alzheimer's disease and MCI, further research is undoubtedly necessary to provide insight into the association between white matter degeneration and other disease hallmarks. To this end, FBA, in conjunction with other neuroimaging methods, could enable much more fibre tract-specific insight than has previously been possible. Future work should thus probe the fixel-based changes within fibre structures connecting regions of pathological injury detected by other imaging modalities, be they microvascular insults, neurofibrillary pathology, or grey matter atrophy.

Conclusion

Our findings suggest that Alzheimer's disease patients exhibit a characteristic pattern of fibre tract degeneration, which manifests both as microstructural and macrostructural reductions in white matter. The pattern of reductions in structural connectivity is consistent with functional disconnections reported in previous literature, and our findings provide support of a structural basis to network disconnection theories. However, the extent to which white matter degeneration is related to amyloid-β pathology is unclear, and our findings in MCI patients suggest that degeneration may be more closely associated with clinical symptomatology than to abnormal accumulation of amyloid-β. To build a more comprehensive understanding of the pathogenic mechanisms and the association between various pathological insults in Alzheimer's disease, future work incorporating fixel-based analysis is likely to be highly insightful.

Acknowledgements

We thank the patients, researchers and clinicians involved in the Australian Imaging, Biomarkers and Lifestyle (AIBL) study of ageing, and Dr Vincent Doré for his assistance in coordinating data access for this project.

Funding

We are grateful to the National Health and Medical Research Council (NHMRC) of Australia and the Victorian Government's Operational Infrastructure

Support Program for their funding support. V.V. is supported by an NHMRC Research Fellowship (1046571). R.M. is supported by a Melbourne International Research Scholarship from the University of Melbourne and Yulgibar Alzheimer's Research Program Award.

Supplementary material

Supplementary material is available at *Brain* online.

References

Acosta-Cabronero J, Williams GB, Pengas G, Nestor PJ. Absolute diffusivities define the landscape of white matter degeneration in Alzheimer's disease. Brain 2010; 133: 529–39.

Agosta F, Pievani M, Geroldi C, Copetti M, Frisoni GB, Filippi M. Resting state fMRI in Alzheimer's disease: beyond the default mode network. Neurobiol Aging 2012; 33: 1564–78.

Aizenstein HJ, Nebes RD, Saxton JA, Price JC, Mathis CA, Tsopelas ND, et al. Frequent amyloid deposition without significant cognitive impairment among the elderly. Arch Neurol 2008; 65: 1509–17.

Alexander GE, Chen K, Pietrini P, Rapoport SI, Reiman EM. Longitudinal PET evaluation of cerebral metabolic decline in dementia: a potential outcome measure in Alzheimer's disease treatment studies. Am J Psychiatry 2002; 159: 738–45.

Altamura C, Scrascia F, Quattrocchi CC, Errante Y, Gangemi E, Curcio G, et al. Regional MRI diffusion, white-matter hyperintensities, and cognitive function in Alzheimer's disease and vascular dementia. J Clin Neurol 2016; 12: 201–8.

Andersson JLR, Sotiropoulos SN. An integrated approach to correction for off-resonance effects and subject movement in diffusion MR imaging. Neuroimage 2016; 125: 1063–78.

Assaf Y, Basser PJ. Composite hindered and restricted model of diffusion (CHARMED) MR imaging of the human brain. Neuroimage 2005; 27: 48–58.

Bach M, Laun FB, Leemans A, Tax CMW, Biessels GJ, Stieltjes B, et al. Methodological considerations on tract-based spatial statistics (TBSS). Neuroimage 2014; 100: 358–69.

Behrens T, Berg HJ, Jbabdi S, Rushworth M, Woolrich MW. Probabilistic diffusion tractography with multiple fibre orientations: what can we gain? Neuroimage 2007; 34: 144–55.

Bosch B, Arenaza-Urquijo EM, Rami L, Sala-Llonch R, Junque C, Sole-Padulles C, et al. Multiple DTI index analysis in normal aging, amnestic MCI and AD. Relationship with neuropsychological performance. Neurobiol Aging 2012; 33: 61–74.

Brickman AM. Contemplating Alzheimer's disease and the contribution of white matter hyperintensities. Curr Neurol Neurosci Rep 2013; 13: 415.

Brier MR, Thomas JB, Ances BM. Network dysfunction in Alzheimer's disease: refining the disconnection hypothesis. Brain Connect 2014; 4: 299–311.

Brun A, Englund E. A white matter disorder in dementia of the Alzheimer type: a pathoanatomical study. Ann Neurol 1986; 19: 253–62.

Buckner RL, Sepulcre J, Talukdar T, Krienen FM, Liu H, Hedden T, et al. Cortical hubs revealed by intrinsic functional connectivity: mapping, assessment of stability, and relation to Alzheimer's disease. J Neurosci 2009; 29: 1860–73.

Buckner RL, Snyder AZ, Shannon BJ, LaRossa G, Sachs R, Fotenos AF, et al. Molecular, structural, and functional characterization of Alzheimer's disease: evidence for a relationship between default activity, amyloid, and memory. J Neurosci 2005; 25: 7709–17.

Canter RG, Penney J, Tsai L-H. The road to restoring neural circuits for the treatment of Alzheimer's disease. Nature 2016; 539: 187–96.

Carmichael ST, Price JL. Limbic connections of the orbital and medial prefrontal cortex in macaque monkeys. J Comp Neurol 1995; 363: 615–41.

Castellani RJ, Perry G. Pathogenesis and disease-modifying therapy in Alzheimer's disease: the flat line of progress. Arch Med Res 2012; 43: 694–8.

Chua TC, Wen W, Slavin MJ, Sachdev PS. Diffusion tensor imaging in mild cognitive impairment and Alzheimer's disease: a review. Curr Opin Neurol 2008; 21: 83–92.

Damoiseaux JS, Smith SM, Witter MP, Sanz-Arigita EJ, Barkhof F, Scheltens P, et al. White matter tract integrity in aging and Alzheimer's disease. Hum Brain Mapp 2009; 30: 1051–9.

De Lacoste MC, Kirkpatrick JB, Ross ED. Topography of the human corpus callosum. J Neuropathol Exp Neurol 1985; 44: 578–91.

Delbeuck X, Van der Linden M, Collette F. Alzheimer's disease as a disconnection syndrome? Neuropsychol Rev 2003; 13: 79–92.

Dhollander T, Connelly A. A novel iterative approach to reap the benefits of multi-tissue CSD from just single-shell (+ b = 0) diffusion MRI data. In: 24th International Society of Magnetic Resonance in Medicine, vol. 24. Singapore; 2016, p. 3010.

Dhollander T, Raffelt D, Connelly A. Towards interpretation of 3-tissue constrained spherical deconvolution results in pathology. In: 25th International Society of Magnetic Resonance in Medicine, vol. 25. Honolulu, Hawaii; 2017, p. 1815.

Dhollander T, Raffelt D, Connelly A. Unsupervised 3-tissue response function estimation from single-shell or multi-shell diffusion MR data without a co-registered T1 image. Proceedings of ISMRM Workshop on Breaking the Barriers of Diffusion MRI. Lisbon, Portugal; 2016, p. 5.

Doan NT, Engvig A, Persson K, Alnæs D, Kaufmann T, Rokicki J, et al. Dissociable diffusion MRI patterns of white matter microstructure and connectivity in Alzheimer's disease spectrum. Sci Rep 2017; 7: 45131.

Douaud G, Jbabdi S, Behrens TEJ, Menke RA, Gass A, Monsch AU, et al. DTI measures in crossing-fibre areas: increased diffusion anisotropy reveals early white matter alteration in MCI and mild Alzheimer's disease. Neuroimage 2011; 55: 880–90.

Drzezga A, Lautenschlager N, Siebner H, Riemenschneider M, Willoch F, Minoshima S, et al. Cerebral metabolic changes accompanying conversion of mild cognitive impairment into Alzheimer's disease: a PET follow-up study. Eur J Nucl Med Mol Imaging 2003; 30: 1104–13.

Ellis KA, Bush AI, Darby D, De Fazio D, Foster J, Hudson P, et al. The Australian Imaging, Biomarkers and Lifestyle (AIBL) study of aging: methodology and baseline characteristics of 1112 individuals recruited for a longitudinal study of Alzheimer's disease. Int Psychogeriatr 2009; 21: 672–87.

Englund E, Brun A, Alling C. White matter changes in dementia of Alzheimer's type. Brain 1988; 111: 1425–39.

Fellgiebel A, Müller MJ, Wille P, Dellani PR, Scheurich A, Schmidt LG, et al. Color-coded diffusion-tensor-imaging of posterior cingulate fiber tracts in mild cognitive impairment. Neurobiol Aging 2005; 26: 1193–8.

Frost B, Diamond MI. Prion-like mechanisms in neurodegenerative diseases. Nat Rev Neurosci 2010; 11: 155–9.

Gajamange S, Raffelt D, Dhollander T, Lui E, van der Walt A, Kilpatrick T, et al. Fibre-specific white matter changes in multiple sclerosis patients with optic neuritis. Neuroimage Clin 2018; 17: 60–8.

Gauthier S, Reisberg B, Zaudig M, Petersen RC, Ritchie K, Broich K, et al. Mild cognitive impairment. Lancet 2006; 367: 1262–70.

Genc S, Seal ML, Dhollander T, Malpas CB, Hazell P, Silk TJ. White matter alterations at pubertal onset. Neuroimage 2017; 156: 286–92.

Giacobini E, Gold G. Alzheimer disease therapy—moving from amyloid-β to tau. Nat Rev Neurol 2013; 9: 677–86.

Gold BT, Johnson NF, Powell DK, Smith CD. White matter integrity and vulnerability to Alzheimer's disease: preliminary findings and future directions. Biochim Biophys Acta 2012; 1822: 416–22.

Greicius MD, Srivastava G, Reiss AL, Menon V. Default-mode network activity distinguishes Alzheimer's disease from healthy aging: evidence from functional MRI. Proc Natl Acad Sci USA 2004; 101: 4637–42.

Greicius MD, Supekar K, Menon V, Dougherty RF. Resting-state functional connectivity reflects structural connectivity in the default mode network. Cereb Cortex 2009; 19: 72–8.

Hardy J, Selkoe DJ. The amyloid hypothesis of Alzheimer's disease: progress and problems on the road to therapeutics. Science 2002; 297: 353–6.

Hau J, Sarubbo S, Perchey G, Crivello F, Zago L, Mellet E, et al. Cortical terminations of the inferior fronto-occipital and uncinate fasciculi: anatomical stem-based virtual dissection. Front Neuroanat 2016; 10: 58.

van den Heuvel M, Mandl R, Luigjes J, Hulshoff Pol H. Microstructural organization of the cingulum tract and the level of default mode functional connectivity. J Neurosci 2008; 28: 10844–51.

Jack CR, Knopman DS, Jagust WJ, Shaw LM, Aisen PS, Weiner MW, et al. Hypothetical model of dynamic biomarkers of the Alzheimer's pathological cascade. Lancet Neurol 2010; 9: 119–28.

Jeurissen B, Leemans A, Tournier J, Jones DK, Sijbers J. Investigating the prevalence of complex fiber configurations in white matter tissue with diffusion magnetic resonance imaging. Hum Brain Mapp 2013; 34: 2747–66.

Jicha GA, Parisi JE, Dickson DW, Johnson K, Cha R, Ivnik RJ, et al. Neuropathologic outcome of mild cognitive impairment following progression to clinical dementia. Arch Neurol 2006; 63: 674–81.

Jones DK. Challenges and limitations of quantifying brain connectivity *in vivo* with diffusion MRI. Imaging Med 2010; 2: 341–55.

Jones DK, Christiansen KF, Chapman RJ, Aggleton JP. Distinct subdivisions of the cingulum bundle revealed by diffusion MRI fibre tracking: implications for neuropsychological investigations. Neuropsychologia 2013a; 51: 67–78.

Jones DK, Knösche TR, Turner R. White matter integrity, fiber count, and other fallacies: the do's and don'ts of diffusion MRI. Neuroimage 2013b; 73: 239–54.

Jones DT, Knopman DS, Gunter JL, Graff-Radford J, Vemuri P, Boeve BF, et al. Cascading network failure across the Alzheimer's disease spectrum. Brain 2016; 139: 547–62.

Larrieu S, Letenneur L, Orgogozo JM, Fabrigoule C, Amieva H, Le Carret N, et al. Incidence and outcome of mild cognitive impairment in a population-based prospective cohort. Neurology 2002; 59: 1594–9.

Lee SH, Coutu JP, Wilkens P, Yendiki A, Rosas HD, Salat DH. Tract-based analysis of white matter degeneration in Alzheimer's disease. Neuroscience 2015; 301: 79–89.

Leyton CE, Villemagne VL, Savage S, Pike KE, Ballard KJ, Piguet O, et al. Subtypes of progressive aphasia: application of the International Consensus Criteria and validation using β-amyloid imaging. Brain 2011; 134: 3030–43.

Mak E, Gabel S, Mirette H, Su L, Williams GB, Waldman A, et al. Structural neuroimaging in preclinical dementia: from microstructural deficits and grey matter atrophy to macroscale connectomic changes. Ageing Res Rev 2017; 35: 250–64.

Minoshima S, Giordani B, Berent S, Frey KA, Foster NL, Kuhl DE. Metabolic reduction in the posterior cingulate cortex in very early Alzheimer's disease. Ann Neurol 1997; 42: 85–94.

Mintun MA, Larossa GN, Sheline YI, Dence CS, Lee SY, Mach RH, et al. [11C] PIB in a nondemented population Potential antecedent marker of Alzheimer disease. Neurology 2006; 67: 446–52.

Mitchell AJ, Shiri-Feshki M. Rate of progression of mild cognitive impairment to dementia–meta-analysis of 41 robust inception cohort studies. Acta Psychiatr Scand 2009; 119: 252–65.

Mori S, Wakana S, van Zijl PCM, Nagae-Poetscher LM. MRI atlas of human white matter. Burlington: Elsevier Science; 2005.

Nakata Y, Sato N, Abe O, Shikakura S, Arima K, Furuta N, et al. Diffusion abnormality in posterior cingulate fiber tracts in Alzheimer's disease: tract-specific analysis. Radiat Med 2008; 26: 466–73.

Nestor PJ, Fryer TD, Smielewski P, Hodges JR. Limbic hypometabolism in Alzheimer's disease and mild cognitive impairment. Ann Neurol 2003; 54: 343–51.

Nichols TE, Holmes AP. Nonparametric permutation tests for functional neuroimaging: a primer with examples. Hum Brain Mapp 2002; 15: 1–25.

Oishi K, Faria A, Jiang H, Li X, Akhter K, Zhang J, et al. Atlas-based whole brain white matter analysis using large deformation diffeomorphic metric mapping: application to normal elderly and Alzheimer's disease participants. Neuroimage 2009; 46: 486–99.

Palop JJ, Chin J, Mucke L. A network dysfunction perspective on neurodegenerative diseases. Nature 2006; 443: 768–73.

Pengas G, Hodges JR, Watson P, Nestor PJ. Focal posterior cingulate atrophy in incipient Alzheimer's disease. Neurobiol Aging 2010; 31: 25–33.

Petersen RC. Mild cognitive impairment as a diagnostic entity. J Intern Med 2004; 256: 183–94.

Petersen RC, Smith GE, Waring SC, Ivnik RJ, Tangalos EG, Kokmen E. Mild cognitive impairment: clinical characterization and outcome. Arch Neurol 1999; 56: 303–8.

Petrides M, Pandya DN. Efferent association pathways from the rostral prefrontal cortex in the macaque monkey. J Neurosci 2007; 27: 11573–86.

Pierpaoli C, Basser PJ. Toward a quantitative assessment of diffusion anisotropy. Magn Reson Med 1996; 36: 893–906.

Rabinovici GD, Jagust WJ, Furst AJ, Ogar JM, Racine CA, Mormino EC, et al. Abeta amyloid and glucose metabolism in three variants of primary progressive aphasia. Ann Neurol 2008; 64: 388–401.

Raffelt DA, Smith RE, Ridgway GR, Tournier J-D, Vaughan DN, Rose S, et al. Connectivity-based fixel enhancement: whole-brain statistical analysis of diffusion MRI measures in the presence of crossing fibres. Neuroimage 2015; 117: 40–55.

Raffelt DA, Tournier J-D, Smith RE, Vaughan DN, Jackson G, Ridgway GR, et al. Investigating white matter fibre density and morphology using fixel-based analysis. Neuroimage 2017; 144: 58–73.

Raffelt D, Tournier J-D, Crozier S, Connelly A, Salvado O. Reorientation of fiber orientation distributions using apodized point spread functions. Magn Reson Med 2012a; 67: 844–55.

Raffelt D, Tournier J-D, Fripp J, Crozier S, Connelly A, Salvado O. Symmetric diffeomorphic registration of fibre orientation distributions. Neuroimage 2011; 56: 1171–80.

Raffelt D, Tournier J-D, Rose S, Ridgway GR, Henderson R, Crozier S, et al. Apparent fibre density: a novel measure for the analysis of diffusion-weighted magnetic resonance images. Neuroimage 2012b; 59: 3976–94.

Raj A, Kuceyeski A, Weiner M. A network diffusion model of disease progression in dementia. Neuron 2012; 73: 1204–15.

Reijmer YD, Leemans A, Heringa SM, Wielaard I, Jeurissen B, Koek HL, et al. Improved sensitivity to cerebral white matter abnormalities in Alzheimer's disease with spherical deconvolution based tractography. PLoS One 2012; 7: e44074.

Rodrigue KM, Kennedy KM, Devous MD Sr, Rieck JR, Hebrank AC, Diaz-Arrastia R, et al. β-Amyloid burden in healthy aging regional distribution and cognitive consequences. Neurology 2012; 78: 387–95.

Rose SE, Chen F, Chalk JB, Zelaya FO, Strugnell WE, Benson M, et al. Loss of connectivity in Alzheimer's disease: an evaluation of white matter tract integrity with colour coded MR diffusion tensor imaging. J Neurol Neurosurg Psychiatry 2000; 69: 528–30.

Rowe CC, Bourgeat P, Ellis KA, Brown B, Lim YY, Mulligan R, et al. Predicting Alzheimer disease with β-amyloid imaging: results from

the Australian imaging, biomarkers, and lifestyle study of ageing. Ann Neurol 2013; 74: 905–13.
Rowe CC, Ellis KA, Rimajova M, Bourgeat P, Pike KE, Jones G, et al. Amyloid imaging results from the Australian Imaging, Biomarkers and Lifestyle (AIBL) study of aging. Neurobiol Aging 2010; 31: 1275–83.
Schwarz CG, Reid RI, Gunter JL, Senjem ML, Przybelski SA, Zuk SM, et al. Improved DTI registration allows voxel-based analysis that outperforms tract-based spatial statistics. Neuroimage 2014; 94: 65–78.
Seeley WW, Crawford RK, Zhou J, Miller BL, Greicius MD. Neurodegenerative diseases target large-scale human brain networks. Neuron 2009; 62: 42–52.
Sexton CE, Kalu UG, Filippini N, Mackay CE, Ebmeier KP. A meta-analysis of diffusion tensor imaging in mild cognitive impairment and Alzheimer's disease. Neurobiol Aging 2011; 32: 2322.e5–e18.
Smith RE, Tournier J-D, Calamante F, Connelly A. SIFT: spherical-deconvolution informed filtering of tractograms. Neuroimage 2013; 67: 298–312.
Smith SM, Jenkinson M, Johansen-Berg H, Rueckert D, Nichols TE, Mackay CE, et al. Tract-based spatial statistics: voxelwise analysis of multi-subject diffusion data. Neuroimage 2006; 31: 1487–505.
Smith SM, Nichols TE. Threshold-free cluster enhancement: addressing problems of smoothing, threshold dependence and localisation in cluster inference. Neuroimage 2009; 44: 83–98.
Taoka T, Iwasaki S, Sakamoto M, Nakagawa H, Fukusumi A, Myochin K, et al. Diffusion anisotropy and diffusivity of white matter tracts within the temporal stem in Alzheimer disease: evaluation of the 'tract of interest' by diffusion tensor tractography. AJNR Am J Neuroradiol 2006; 27: 1040–5.
Taylor ANW, Kambeitz-Ilankovic L, Gesierich B, Simon-Vermot L, Franzmeier N, Araque Caballero MÁ, et al. Tract-specific white matter hyperintensities disrupt neural network function in Alzheimer's disease. Alzheimers Dement 2017; 13: 225–35.
Teipel SJ, Bokde ALW, Meindl T, Amaro E Jr, Soldner J, Reiser MF, et al. White matter microstructure underlying default mode network connectivity in the human brain. Neuroimage 2010; 49: 2021–32.
Thal DR, Attems J, Ewers M. Spreading of amyloid, tau, and microvascular pathology in Alzheimer's disease: findings from neuropathological and neuroimaging studies. J Alzheimers Dis 2014; 42 (Suppl 4): S421–9.
Tournier J-D, Calamante F, Connelly A. Robust determination of the fibre orientation distribution in diffusion MRI: non-negativity constrained super-resolved spherical deconvolution. Neuroimage 2007; 35: 1459–72.
Tournier J-D, Calamante F, Gadian DG, Connelly A. Direct estimation of the fiber orientation density function from diffusion-weighted MRI data using spherical deconvolution. Neuroimage 2004; 23: 1176–85.
Tustison NJ, Avants BB, Cook PA, Zheng Y, Egan A, Yushkevich PA, et al. N4ITK: improved N3 bias correction. IEEE Trans Med Imaging 2010; 29: 1310–20.
Vaughan DN, Raffelt D, Curwood E, Tsai M-H, Tournier J-D, Connelly A, et al. Tract-specific atrophy in focal epilepsy: disease, genetics, or seizures? Ann Neurol 2017; 81: 240–50.
Veraart J, Fieremans E, Novikov DS. Diffusion MRI noise mapping using random matrix theory. Magn Reson Med 2016; 76: 1582–93.
Vernooij MW, de Groot M, van der Lugt A, Ikram MA, Krestin GP, Hofman A, et al. White matter atrophy and lesion formation explain the loss of structural integrity of white matter in aging. Neuroimage 2008; 43: 470–77.
Villain N, Desgranges B, Viader F, de la Sayette V, Mézenge F, Landeau B, et al. Relationships between hippocampal atrophy, white matter disruption, and gray matter hypometabolism in Alzheimer's disease. J Neurosci 2008; 28: 6174–81.
Villemagne VL, Burnham S, Bourgeat P, Brown B, Ellis KA, Salvado O, et al. Amyloid β deposition, neurodegeneration, and cognitive decline in sporadic Alzheimer's disease: a prospective cohort study. Lancet Neurol 2013; 12: 357–67.
Wakana S, Jiang H, Nagae-Poetscher LM, van Zijl PCM, Mori S. Fiber tract–based atlas of human white matter anatomy. Radiology 2004; 230: 77–87.
Wang T, Shi F, Jin Y, Yap P-T, Wee C-Y, Zhang J, et al. Multilevel deficiency of white matter connectivity networks in Alzheimer's disease: a diffusion MRI study with DTI and HARDI models. Neural Plast 2016; 2016: 2947136.
Wardlaw JM, Smith EE, Biessels GJ, Cordonnier C, Fazekas F, Frayne R, et al. Neuroimaging standards for research into small vessel disease and its contribution to ageing and neurodegeneration. Lancet Neurol 2013; 12: 822–38.
Winblad B, Palmer K, Kivipelto M, Jelic V, Fratiglioni L, Wahlund L-O, et al. Mild cognitive impairment–beyond controversies, towards a consensus: report of the International Working Group on Mild Cognitive Impairment. J Intern Med 2004; 256: 240–6.
Wright DK, Johnston LA, Kershaw J, Ordidge R, O'Brien TJ, Shultz SR. Changes in apparent fiber density and track-weighted imaging metrics in white matter following experimental traumatic brain injury. J Neurotrauma 2017; 34: 2109–118.
Wu Y, Sun D, Wang Y, Wang Y, Ou S. Segmentation of the cingulum bundle in the human brain: a new perspective based on DSI tractography and fiber dissection study. Front Neuroanat 2016; 10: 84.
Yoshita M, Fletcher E, Harvey D, Ortega M, Martinez O, Mungas DM, et al. Extent and distribution of white matter hyperintensities in normal aging, MCI, and AD. Neurology 2006; 67: 2192–8.
Zhang Y, Schuff N, Jahng G-H, Bayne W, Mori S, Schad L, et al. Diffusion tensor imaging of cingulum fibers in mild cognitive impairment and Alzheimer disease. Neurology 2007; 68: 13–19.
Zhang Y, Zhang J, Oishi K, Faria AV, Jiang H, Li X, et al. Atlas-guided tract reconstruction for automated and comprehensive examination of the white matter anatomy. Neuroimage 2010; 52: 1289–301.
Zhou J, Gennatas ED, Kramer JH, Miller BL, Seeley WW. Predicting regional neurodegeneration from the healthy brain functional connectome. Neuron 2012; 73: 1216–27.